

WIDE-ANGLE POLARIZATION-INDEPENDENT PLANAR LEFT-HANDED METAMATERIALS BASED ON DIELECTRIC RESONATORS

J. F. Wang, S. B. Qu, H. Ma, Y. M. Yang, and X. Wu

The College of Science
Air Force Engineering University
Xi'an, Shaanxi 710051, China

Z. Xu

Electronic Materials Research Laboratory
Key Laboratory of the Ministry of Education
Xi'an Jiaotong University
Xi'an, Shaanxi 710049, China

M. J. Hao

Northwest University
Xi'an, Shaanxi 710127, China

Abstract—Based on dielectric resonators, the design and implementation of planar left-handed metamaterials made of dielectric blocks are investigated in this paper. By etching simple metallic patterns on surface of the dielectric blocks, field distributions of the desired resonance modes can be enhanced while those of the undesired are suppressed. In this way, the resonance frequency of the desired mode can be tuned down to lower frequency range. A wide-angle polarization-independent planar left-handed metamaterial based on disk-like dielectric resonators is proposed and analyzed. Such a left-handed metamaterial is independent of the polarization of incident waves. Moreover, its double-negative property keeps almost the same under a wide range of incident angles. At the end, practical implementation of the left-handed metamaterial by using flexible supporting slabs is given. Due to its polarization-independence, wide range of incident angle and high flexibility, the proposed left-handed metamaterial is ready to be used in various microwave components, such as antenna radomes, microwave filters and frequency selective surfaces.

Corresponding author: J. F. Wang (wangjiafu1981@126.com).

1. INTRODUCTION

Left-handed metamaterials (LHMs) with simultaneously negative permeability and permittivity have been attracting great attentions since the initiatory work of Pendry and Smith [1, 2]. Due to their unique electromagnetic properties, LHMs have great potential application values in many fields. Because of this, many scientists from different research fields have done a lot of work for the development of LHMs. A great variety of LHMs have been envisioned and fabricated. Similar to the working principle of the structure in [2], dielectric-metallic LHM unit cells, such as S-shaped [3], Ω -shaped [4], coplanar magnetic and electric resonator unit cells [5], have been proposed. Nevertheless, there is an annoying problem for the above-mentioned unit cells. Incident waves must be in parallel with the substrate plane, which make it quite troublesome to be fabricated and used. With an aim to overcome this problem, planar LHMs, which allow the incident waves to be perpendicular to the substrate plane, were proposed and fabricated [6–11]. Typical planar LHMs are the fishnet structures proposed by Soukoulis et al. [9].

Recently, many researchers are focusing on all-dielectric realization of LHMs [12–18]. Many all-dielectric LHM unit cells, such as binary spherical [12], cubic [13] and disk-like unit cells [14], were proposed. These unit cells are based on different resonance modes in the unit cells which behave like dielectric resonators. Under a certain resonance mode, the effective permeability or/and permittivity are negative. The key to realizing all-dielectric metamaterials is to get the proper resonance modes. High-dielectric constant ceramics with good temperature stability and low dielectric loss are required to guarantee the long-wavelength condition. However, to date, dielectric constants of microwave ceramic materials, such as $\text{Ba}_2\text{Ti}_9\text{O}_{20}$, BaTi_4O_9 , $\text{BaO-PbO-Nd}_2\text{O}_3\text{-TiO}_2$, are mostly between $30 \sim 100$, much less than some all-dielectric unit cells require [16, 17]. For many all-dielectric unit cells, their first resonance frequencies are effective medium theory cannot be used to characterize them. Only when the wavelength is at least ten times larger than the unit cell size can the effective medium theory be used to characterize them. In order to obtain longer wavelength, resonance frequency must be reduced. As a result, it is desirable to design unit cells whose resonance modes can be tuned down to lower frequencies.

In this paper, planar LHMs based on dielectric resonators were proposed. As a typical example, planar LHMs based on disk-like dielectric resonators are investigated. By etching a circular metallic ring on each end face of the dielectric resonator unit cell, the first

resonance can be tuned significantly down to lower frequency range so as to meet the long-wavelength condition. Thus, the LHM can be described by effective medium theory. Since the cross section of the disk-like dielectric resonator as well as the metallic ring are all circular, the magnetic metamaterial is independent of the polarization of incident waves. Under a wide incident angle range, the double-negative frequency range keeps almost the same. Practical implementation of the proposed LHM by using flexible low-dielectric supporting slabs is also given. The proposed planar LHM owes its advantages to wide-angle incidence and polarization independence.

2. TUNING RESONANCE FREQUENCIES BY METALLIC PATTERNS

2.1. Resonance Frequencies of Bare Dielectric Resonators

Only recently, materials having a dielectric constant between 30 and 100 with good temperature stability and low dielectric losses have become available. This greatly facilitates the design of all-dielectric LHMs, but the dielectric constants of commercially available ceramic materials are still not high enough to meet the requirement of some unit cells [16, 17]. This leads to a comparatively high resonance frequency. Thus, long-wavelength condition can not be satisfied and the corresponding LHMs cannot be characterized by the effective medium theory. As a result, it is necessary to tune the desired resonance mode down to lower frequency ranges. All-dielectric LHMs are always made of high-dielectric ceramic materials, no matter what shapes of the unit cells are. A high-dielectric block can be regarded as a dielectric resonator, so we can design and tune all-dielectric LHMs by the same methods used in designing dielectric resonators. Usually, some certain metallic patterns are etched on the surface of dielectric resonators to enhance desired modes or to suppress undesired modes. Based on this idea, magnetic or/and electric resonances can be tuned by using metallic patterns so as to design new kinds of metamaterials.

For an isolated disk-like dielectric resonator shown in Figure 1(a), the resonance mode with the lowest resonance frequency is the $TE_{01\delta}$ mode. According to the electric and magnetic field distributions shown in Figures 1(b) and (c), the resonator behaves like a magnetic dipole in $TE_{01\delta}$ mode. Since the electric and magnetic dipole moments can be envisioned as the alphabet for making metamaterials [14], the resonator is expected to be a magnetic metamaterial in the $TE_{01\delta}$ mode. Although the geometrical form of a dielectric resonator is extremely simple, an exact solution of the Maxwell equations is considerably more difficult than for hollow metal cavities. For this

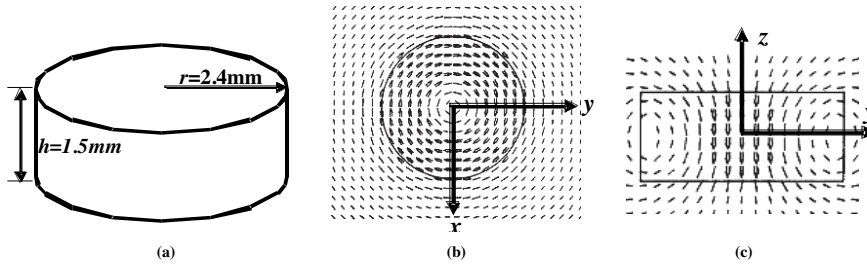


Figure 1. An isolated disk-like dielectric resonator (a) and its electric field distribution in (x, y) plane (b), magnetic field distribution in (y, z) plane (c) for $TE_{01\delta}$ mode.

reason, the exact resonant frequency of a certain resonant mode, such as $TE_{01\delta}$ mode, can only be computed by rather complicated numerical procedures. For an approximate estimation of the resonant frequency of the isolated dielectric resonator, the following simple formula [19] can be used

$$f_{\text{GHz}} = \frac{34}{r_{\text{mm}} \sqrt{\varepsilon_r}} \left(\frac{r}{h} + 3.45 \right) \quad (1)$$

The radius of the resonator is denoted by r and its height by h . The lengths are expressed in millimeters, and the frequency in gigahertz. The relative dielectric constant of the material is ε_r . The above formula is accurate to about 2% in the range

$$0.5 < r/h < 2 \quad \text{and} \quad 30 < \varepsilon_r < 50 \quad (2)$$

The dielectric resonator we consider in this paper as an example is made of BaTi_4O_9 whose dielectric constant $\varepsilon_r = 39.2$, loss tangent $\tan \delta = 0.0001$ and temperature coefficient $T_f = +4 \text{ ppm}/^\circ\text{C}$. The radius and height of the resonator are $r = 2.4 \text{ mm}$ and $h = 1.5 \text{ mm}$, respectively. By using (1) to estimate the first resonance frequency, we obtain

$$f_{\text{GHz}} = \frac{34}{2.4 \times \sqrt{39.2}} \left(\frac{2.4}{1.5} + 3.45 \right) \approx 11.4 \text{ GHz}$$

At 11.4 GHz, the wave-length in free space is about 26.3 mm, only about 5.5 times the diameter of the resonator, so the unit cell cannot be described by effective medium theory. The resonance frequency of the $TE_{01\delta}$ mode has to be tuned down.

2.2. Dielectric Resonator with Circular Metallic Patterns

Figure 2 shows the dielectric resonator unit cell with circular metallic patterns. The unit cell is put into a $5\text{ mm} \times 5\text{ mm} \times 3\text{ mm}$ lattice. Compared with the dielectric resonator shown in Figure 1(a), there are two thin circular copper rings on each end face of the dielectric resonator. The outer radius of the copper ring, the width and thickness of the copper strip are: $r_0 = 2.0\text{ mm}$, $w = 0.2\text{ mm}$, $t = 0.050\text{ mm}$, respectively. From the electric and magnetic field distributions shown in Figures 1(b) and (c), we can find that the electric field is stronger on the outer part of the end faces while the magnetic field is strongest in the center part around the axis. The copper ring is such that it is polarized along the electric field lines while perpendicular to the magnetic field lines. Thus, electric field on the end face and magnetic field pass through the copper ring all contribute to the enhancement of the magnetic resonance, so the resonant frequency of $\text{TE}_{01\delta}$ mode will decrease significantly.

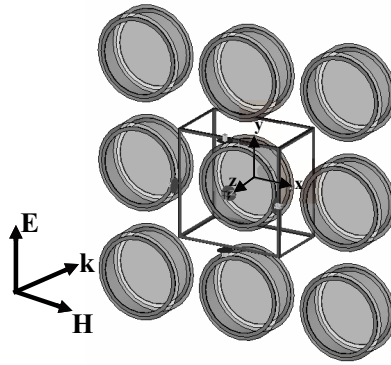


Figure 2. Unit cell of dielectric resonator with copper rings etched on both of the two end faces.

Numerical simulations are carried out using the commercial FDTD solver CST Microwave Studio. As shown in Figure 2, the four lateral boundaries along x and y axes are Periodic Boundaries while the two boundaries along z axis are Open Boundaries. Plane waves are incident onto the unit cell with an incident angle θ with respect to the $-z$ direction. Consider a normally incident plane wave onto the unit cell. Since the lateral boundaries are Periodic Boundaries, the structure shown in Figure 2 is actually one layer of infinite slab made of the unit cell. Because the cross section of the dielectric resonator and the copper ring are all circular, the polarization of the incident plane wave has no influence on its electromagnetic response. Figure 3

shows the simulated transmission spectra of one layer of the proposed metamaterial. As shown in Figure 3, there are two transmission dips in 4~10 GHz, one of which is around 5 GHz and the other around 9 GHz. The two dips indicate two resonances. At 9 GHz, the wavelength in free space is about 33 mm, more than six times larger than the size of the unit cell, so effective medium theory can be employed. This means that we can use effective permeability and permittivity to describe the electromagnetic properties of the infinite magnetic metamaterial slab.

The effective permeability and permittivity can be retrieved from S parameters obtained by simulations or experiments [20, 21]. Figures 4(a) and (b) give the retrieved permeability and permittivity, respectively. Figures 4(a) and (b) show that there is a magnetic resonance around 5.2 GHz while there is an electric resonance around

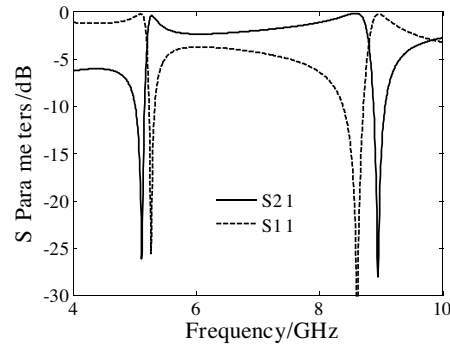


Figure 3. Transmission spectra of one layer of slab made of the unit cell shown in Figure 2.

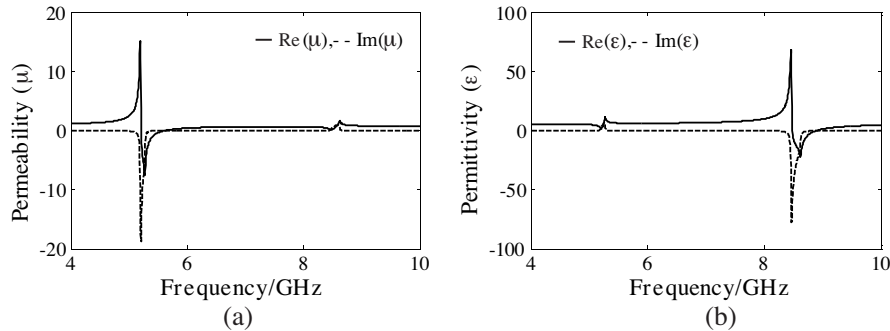


Figure 4. Retrieved constitutive parameters: (a) Effective permeability and (b) effective permittivity for one layer of slab made of the unit cell shown in Figure 1.

8.5 GHz. The real part of effective permeability is negative from 5.2 GHz to 5.6 GHz. Moreover, there is a corresponding anti-resonance [22] of the effective permittivity around 5.2 GHz. The real part of effective permittivity is negative from 8.5 GHz to 9.0 GHz and there is also a corresponding anti-resonance [22] of the effective permeability around 8.5 GHz.

Compared with bare dielectric resonator shown in Figure 1, the first two resonances are significantly tuned down to lower frequency ranges. Of the two resonances, the first one is a magnetic resonance while the second one is an electric resonance. Thus, both magnetic and electric resonances can be tuned down by the circular copper rings.

2.3. Influences of Geometrical Parameters of the Copper Rings

For the proposed unit cell shown in Figure 2, we use the copper ring to tune down the resonance frequency of $TE_{01\delta}$ mode to realize negative permeability at much lower frequency range. Since the field intensity is different on different part of the dielectric resonator, the influence of copper ring is different when its geometrical parameters are changed. Thus, it is necessary to investigate the influence of its geometrical parameters. There are two main geometrical parameters for the copper ring: the outer radius and the strip width, so the influences of the two geometrical parameters were investigated.

Figures 5(a) and (b) show the transmission spectra under different outer radii and strip widths, respectively. As shown in Figure 5(a), as the outer radius decreases, the transmission dip shifts to higher frequencies. This means that the resonance frequency of $TE_{01\delta}$ mode increases as the outer radius decreases. This can be explained by the electric field distribution shown in Figure 1(b). The electric field intensity is stronger on the outer part of the end face while weaker on the inner part. When the outer radius of the copper ring reduces, the electric field coupling to the copper ring becomes weaker. Thus, higher frequency is needed to excite the $TE_{01\delta}$ mode resonance. Figure 5(b) shows that as the strip-width increases, the transmission dip blue-shifts, which means that the magnetic resonance frequency increases with the strip-width. As the strip-width increases, the coupling between the copper ring and the electric field of the dielectric resonator increases, which increases the electric energy while reduces the magnetic energy. Thus, the magnetic field is reduced as the strip-width increases. Again, higher frequency is needed to excite the $TE_{01\delta}$ mode resonance.

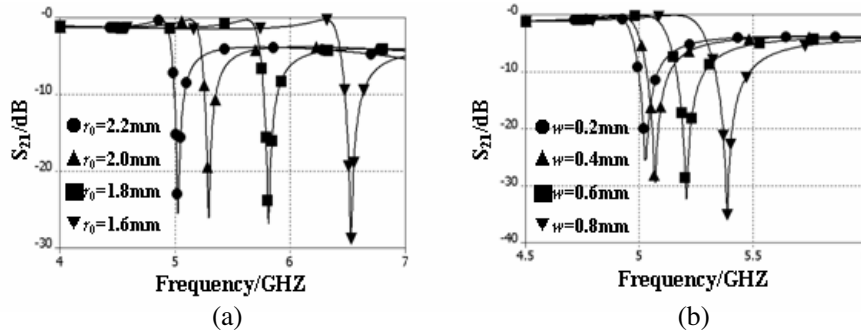


Figure 5. Influences of (a) the outer radius of copper ring and (b) the width of copper strip.

3. LEFT-HANDED METAMATERIALS BASED ON BINARY DIELECTRIC RESONATORS

3.1. The Binary Dielectric Resonator Unit Cell

From the above analysis, we know that resonance frequencies can be tuned down to lower frequency ranges by using copper rings. By changing the radius or the strip width of the copper ring, resonance frequencies can be tuned down to desired ranges. Moreover, both the magnetic and electric resonance can be tuned. Thus, simultaneous magnetic and electric resonances can be realized by tuning the magnetic resonance of one dielectric resonator to the electric resonance range of another dielectric resonator.

Since the magnetic and electric resonances of one dielectric

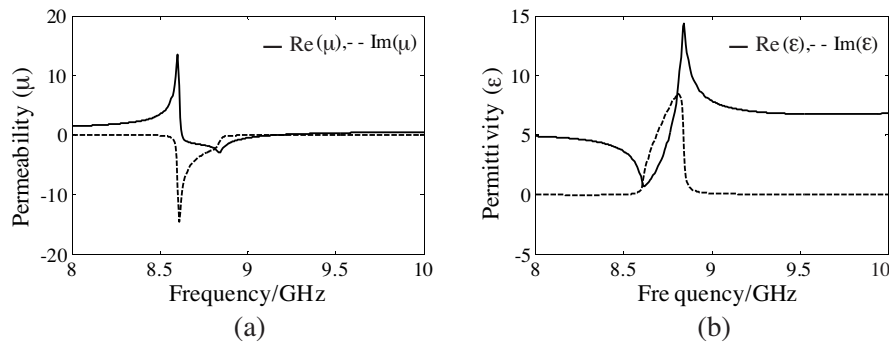


Figure 6. Retrieved effective permeability (a) and permittivity (b) for dielectric resonator with $r_0 = 1$ mm copper rings.

resonator are always separate, two dielectric resonators have to be used. By reducing the radius of the copper rings, magnetic resonance can be tuned upwards to the electric resonance range shown in Figure 5(b). Figures 6(a) and (b) show the retrieved effective permeability and permittivity in 8~10 GHz when the radius of copper rings is reduced to be $r_0 = 1$ mm. For dielectric resonator with $r_0 = 1$ mm copper rings, the real part of its effective permeability is negative in 8.6~9.2 GHz.

Combining the two dielectric resonators with $r_0 = 1$ mm and 2 mm copper rings, both magnetic and electric resonances can be realized at the same frequency range. Figure 7 gives the binary dielectric resonator planar LHM unit cell. For the sake of numerical simulations, the four lateral boundaries are set to be Periodic Boundaries while the two boundaries along z direction are set to be Open Boundaries. Thus, the structure shown in Figure 7 is a planar slab which is infinite in x and y directions. Plane waves are incident onto the unit cell with an incident angle θ with respect to the $-z$ direction.

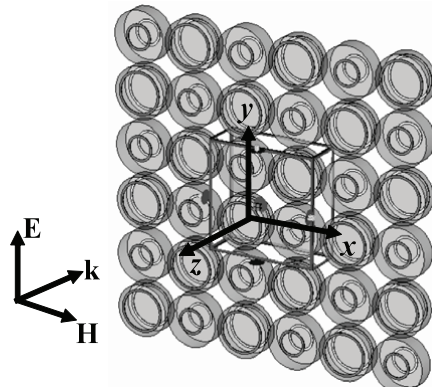


Figure 7. The binary dielectric resonator planar LHM unit cell.

3.2. Simultaneously Negative Permeability and Permittivity under Normal Incidences

Consider the case in which plane waves are incident normally onto the slab shown in Figure 7. In this case, the electric and magnetic vectors of the incident waves are paralleled to the LHM slab while the propagation direction is perpendicular to the LHM slab. From the calculated S parameters, the retrieved parameters are shown in Figure 8. Figures 8(a), (b), (c) and (d) show the retrieved effective permeability, permittivity, relative impedance and refractive index, respectively. As shown in Figures 8(a) and (b), the real part of the

effective permeability is negative in 8.87 ~ 9.12 GHz while that of the effective permittivity is negative in 8.87 ~ 9.17 GHz. In the overlapped frequency range where both real parts of effective permeability and permittivity are negative, a left-handed band is expected. As shown in Figure 8(c), in the frequency range 8.87 ~ 9.12 GHz, real part of the refraction index is negative.

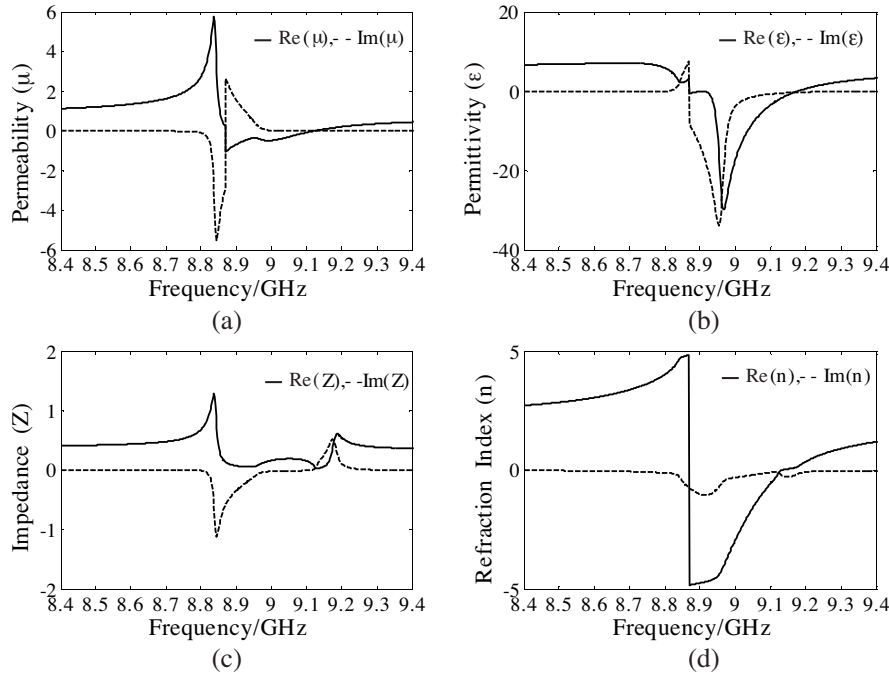


Figure 8. Retrieved effective permeability (a), effective permittivity (b), relative impedance (c) and refraction index (d) for one layer of the proposed LHM slab.

Note that there are some differences between the binary dielectric resonator slab shown in Figure 7 and single dielectric resonator slab shown in Figure 2. Compared with the effective permeability shown in Figure 6, there is a blue-shift for the negative range of effective permeability shown in Figure 8(a). Moreover, the negative permeability bandwidth becomes a bit narrower. Meanwhile, compared with the effective permittivity shown in Figure 4(b), there is also a blue-shift for the negative range of effective permeability shown in Figure 8(b). This can be explained by the interactions between the two kinds of dielectric resonators.

From the retrieved parameters, we can see that LHMs can be

realized by combining two dielectric resonators with different copper rings. For the LHM slab we consider here, negative permeability is realized by the first resonance of the dielectric resonator with $r_0 = 1$ mm copper rings, whereas negative permittivity is realized by the second resonance of the dielectric resonator with $r_0 = 2$ mm copper rings.

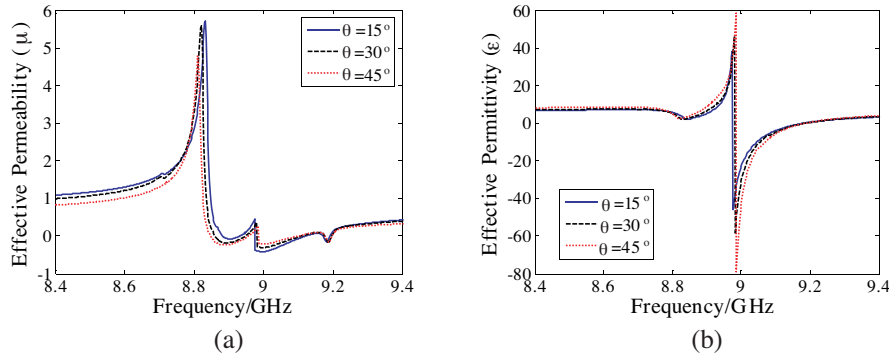


Figure 9. Real parts of retrieved effective permeability (a) and permittivity (b) under different incident angles for TE plane waves.

3.3. Double-negative Property under Oblique Incidences

For oblique incidences, we must consider two cases: incident TE and TM plane waves. In the TE case, the electric vector of incident plane waves keeps paralleled to the LHM slab while the orientation of magnetic vector varies as the incidence angle changes. Figures 9(a) and (b) show the retrieved real parts of effective permeability and permittivity in the TE case, respectively. As shown in Figures 9(a) and (b), both the negative ranges of effective permeability and permittivity shift upwards as the incident angle increases. But the blue-shifts are so minor that they can be neglected. Thus, the LHM slab keeps almost the same left-handed bandwidth under an incidence angle range $0^\circ < \theta < 45^\circ$.

In the TM case, the magnetic vector of incident plane waves keeps paralleled to the LHM slab while the orientation of electric vector varies as the incidence angle changes. Figures 10(a) and (b) give the retrieved real part of the effective permeability and permittivity in the TM case. As the incident angle increases, both of the two negative ranges also shift upwards. Similarly, the blue-shifts are also quite minor, so the LHM slab can be regarded as with the same left-handed properties under a incidence angle $0^\circ < \theta < 30^\circ$ for the TM incident plane waves.

From the above analysis, it can be concluded that the planar LHM slab has approximately the same left-handed properties under an incidence angle varying from 0° to 30° . The wide-angle property of the planar LHM greatly facilitates practical applications.

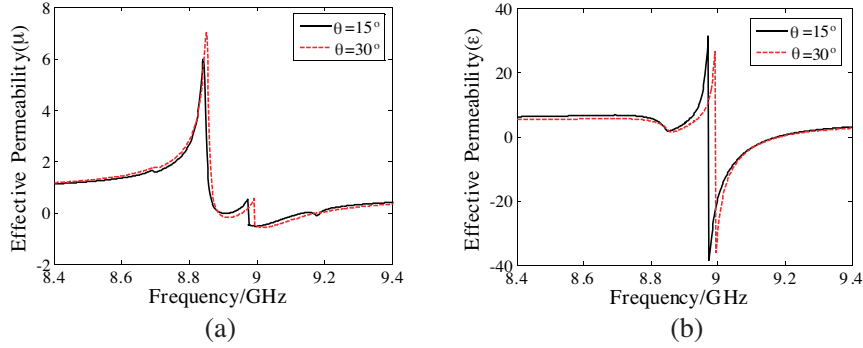


Figure 10. Real parts of retrieved effective permeability (a) and permittivity (b) under different incident angles for TM plane waves.

4. PRACTICAL IMPLEMENTATION

In practice, the unit cells have to be fixed. Some authors chose the method of embedding the high-dielectric blocks into low-dielectric matrix [12–14]. This method is quite demanding, so it is difficult to be used in practice. To avoid such a difficulty, the planar LHM can be realized in practice by two supporting slabs, as shown in Figure 11(a). In order to reduce the influence of the two supporting slabs, materials of supporting slabs must be with low dielectric loss and low dielectric constant. Teflon (PTFE) with a dielectric constant 2.08 and loss angle tangent 0.0004 is chosen to be the material of supporting slabs. Besides its low dielectric loss and low dielectric constant, the flexibility of Teflon is quite good, so the planar LHM can be bent quite freely, which makes it convenient for us to apply the planar LHM.

The influence of the two Teflon supporting slabs on the left-handed properties is also investigated. For one layer of the LHM slab shown in Figure 11(a), the effective permeability and permittivity are shown in Figures 11(b) and (c), respectively. Compared with the effective permeability and permittivity without supporting slabs, the two negative ranges have slight red-shifts. But the red-shift of negative permeability range is larger than that of red-shift of negative permittivity range, so the resulted left-handed band becomes narrower than in the case without supporting slabs.

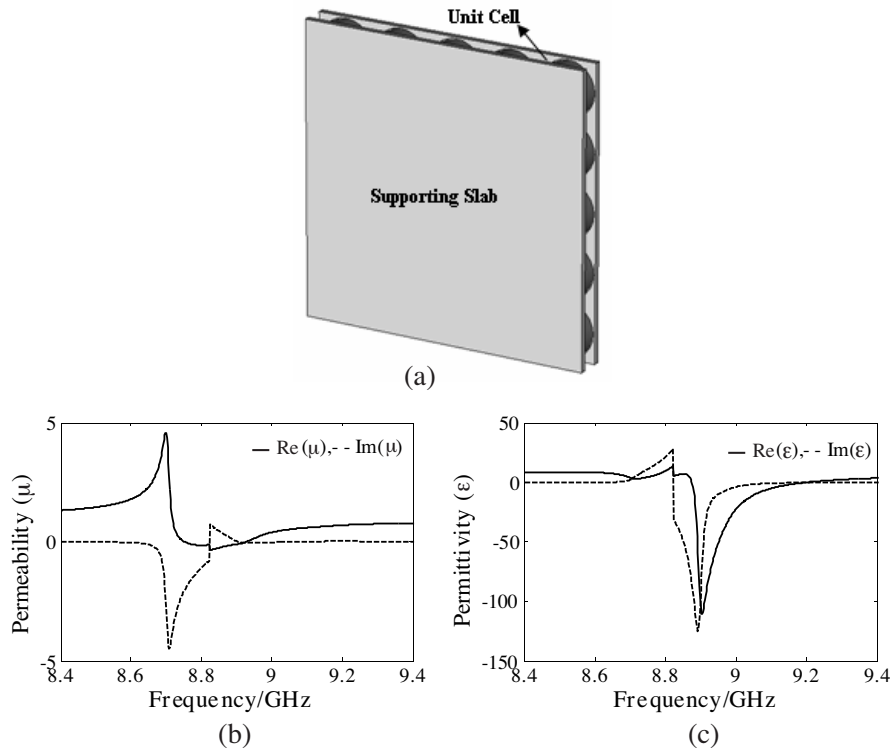


Figure 11. Practical implementation of the proposed magnetic metamaterials: (a) Fixing the unit cells by two supporting slab, (b) retrieved effective permeability, (c) retrieved effective permittivity.

5. CONCLUSIONS

According to the field distributions of different resonance modes of dielectric resonators, metallic patterns can be etched on some special positions on the surface dielectric resonators to adjust the field distributions. Thus, the desired resonance mode can be enhanced while the undesired suppressed. As a result, resonance frequency of the desired modes will be reduced so as to meet the long wavelength condition. Metamaterials with negative permeability and/or negative permittivity can be realized by the desired resonance modes. Since there is many resonance modes for a given dielectric resonator, a great diversity of metamaterial can be designed based on different resonance modes. As a good example, a planar LHM based on disk-like dielectric resonators is designed and analyzed. The proposed planar

LHM meets strictly the long wave-length condition and has almost the same electromagnetic response under a wide range of incidence angles. Because of its high flexibility, wide incidence angle range and polarization independence, the planar LHM is ready to be used in various microwave components, such as antenna radomes, microwave filters and frequency selective surfaces.

ACKNOWLEDGMENT

This work was supported by the National Natural Science Foundation of China (Grant Nos. 50632030 and 60871027).

REFERENCES

1. Pendry, J. B., A. J. Holden, D. J. Robbins, and W. J. Stewart, "Magnetism from conductors and enhanced nonlinear phenomena," *IEEE Trans. Microw. Theory Tech.*, Vol. 47, 2075–2084, 1999.
2. Smith, D. R., W. J. Padilla, D. C. Vier, S. C. Nemat-Nasser, and S. Schultz, "Composite medium with simultaneously negative permeability and permittivity," *Phys. Rev. Lett.*, Vol. 84, 4184–4187, 2000.
3. Xi, S., H. Chen, B.-I. Wu, and J. A. Kong, "Experimental confirmation of guidance properties using planar anisotropic left-handed metamaterial slabs based on S-ring resonators," *Progress In Electromagnetics Research*, PIER 84, 279–287, 2008.
4. Ran, L., J. Huangfu, H. Chen, X. Zhang, K. Cheng, T. M. Grzegorzcyk, and J. A. Kong, "Experimental study on several left-handed metamaterials," *Progress In Electromagnetics Research*, PIER 51, 249–279, 2005.
5. Wang, J. F., S. B. Qu, Z. Xu, J. Q. Zhang, Y. M. Yang, H. Ma, and Ch. Gu, "A candidate three-dimensional GHz left-handed metamaterial composed of coplanar magnetic and electric resonators," *Photon Nanostruct: Fundam Appl.*, Vol. 6, 183, 2008.
6. Zhou, J. F., L. Zhang, G. Tuttle, Th. Koschny, and C. M. Soukoulis, "Negative index materials using simple short wire pairs," *Phys. Rev. B*, Vol. 73, 041101, 2006.
7. Dolling, G., C. Enkrich, M. Wegener, J. F. Zhou, C. M. Soukoulis, and S. Linden, "Cut-wire pairs and plate pairs as magnetic atoms for optical metamaterials," *Opt. Lett.*, Vol. 30, 3198–3200, 2005.
8. Alici, K. B. and E. Ozbay, "A planar metamaterial: Polarization

- independent fishnet structure,” *Photonics Nanostruct: Fundam. Appl.*, Vol. 6, 102–107, 2008.
9. Kafesaki, M., I. Tsiapa, N. Katsarakis, Th. Koschny, C. M. Soukoulis, and E. N. Economou, “Left-handed metamaterials: The fishnet structure and its variations,” *Phys. Rev. B*, Vol. 75, 235114, 2007.
 10. Guven, K., A. O. Cakmak, M. D. Caliskan, T. F. Gundogdu, M. Kafesaki, C. M. Soukoulis, and E. Ozbay, “Bilayer metamaterial: Analysis of left-handed transmission and retrieval of effective medium parameters,” *J. Opt. A: Pure Appl. Opt.*, Vol. 9, 361–365, 2007.
 11. Zhou, J. F., Th. Koschny, L. Zhang, G. Tuttle, and C. M. Soukoulis, “Experimental demonstration of negative index of refraction,” *Appl. Phys. Lett.*, Vol. 88, 221103, 2006.
 12. Holloway, C. L., E. F. Kuester, J. Baker-Jarvis, and P. Kabos, “A double negative (DNG) composite medium composed of magnetodielectric spherical particles embedded in a matrix,” *IEEE Trans. Antennas Propgat.*, Vol. 51, No. 10, 2596–2603, 2003.
 13. Kim, J. and A. Gopinath, “Simulation of a metamaterial containing cubic high dielectric resonators,” *Phys. Rev. B*, Vol. 76, 115126, 2007.
 14. Ahmadi, A. and H. Mosallaei, “Physical configuration and performance modeling of all-dielectric metamaterials,” *Phys. Rev. B*, Vol. 77, 045104, 2008.
 15. Popa, B.-I. and S. A. Cummer, “Compact dielectric particles as a building block for low-loss magnetic metamaterials,” *Phys. Rev. Lett.*, Vol. 100, 207401, 2008.
 16. Peng, L., L. X. Ran, H. S. Chen, H. F. Zhang, J. A. Kong, and T. M. Grzegorzcyk, “Experimental observation of left-handed behavior in an array of standard dielectric resonators,” *Phys. Rev. Lett.*, Vol. 98, 157403, 2007.
 17. Lepetit, T. and E. Akmansoy, “Magnetism in high-contrast dielectric photonic crystals,” *Microwave Opt. Tech. Lett.*, Vol. 50, 909–911, 2008.
 18. Jylhä, L., I. Kolmakov, S. Maslovski, and S. Tretyakova, “Modeling of isotropic backward-wave materials composed of resonant spheres,” *J. Appl. Phys.*, Vol. 99, 043102, 2006.
 19. Kajfez, D. and P. Guillon, Noble Publishing Corporation, Georgia, 1998.
 20. Chen, X. D., T. M. Grzegorzcyk, B.-I. Wu, J. Pacheco, Jr., and J. A. Kong, “Robust method to retrieve the constitutive effective

- parameters of metamaterials,” *Phys. Rev. E*, Vol. 70, 016608, 2004.
21. Smith, D. R., D. C. Vier, Th. Koschny, and C. M. Soukoulis, “Electromagnetic parameter retrieval from inhomogeneous metamaterials,” *Phys. Rev. E*, Vol. 71, 036617, 2005.
 22. Koschny, T., P. Markos, D. R. Smith, and C. M. Soukoulis, “Resonant and antiresonant frequency dependence of the effective parameters of metamaterials,” *Phys. Rev. E*, Vol. 68, 065602, 2003.